

ENGO 623 Inertial Surveying and INS/ GPS Integration

Project 3: INS 3D Reduced Inertial Sensor Mechanization in Local Level Frame

Project report

Submitted by

Ranjeeth Kumar Siddakatte

10119739

PLAN Group, Geomatics Engineering

University of Calgary

1 ABSTRACT

An Inertial Measurement Unit (IMU) used in Inertial Navigation Systems (INS) contains three accelerometers and three gyroscopes (sensors) mounted orthogonal to each other, aligned with the body axis (body frame). The process of mechanization involves integrating the sensor outputs to obtain the user states (position, velocity, attitudes). This project discusses the process of mechanizing with reduced inertial sensor system (RISS) to obtain 3-Dimensional (3D) position, for a land vehicular movement, where the vehicles move mostly in horizontal plane. A brief overview of errors of the outputs of mechanization process is discussed and demonstrated. The performance of 3D-RISS for MEMS grade and tactical grade is compared against the reference. Advantages of 3D-RISS against full IMU mechanization and its drawbacks are also presented.

2 INTRODUCTION

The three accelerometers mounted orthogonally in an IMU measure the linear acceleration of the body in their respective directions. This is integrated to obtain the velocity, which is integrated again to obtain the position. The three gyroscopes mounted in the respective directions of their accelerometers, give the angular velocity vector of the body, which is used to transform the accelerometer outputs from body frame to local level frame. The integration process is recursive. Hence the computed position error due to accelerometer error is proportional to integration time square, t^2 ; similarly, position error due to gyro bias error proportional to t^3 (A. Noureldin, Spring 2013). With many sensors, the complex errors keep growing with time. In case of a 3D-RISS, pitch and roll angles are computed from accelerometers, which makes the error in their angles proportional to t^2 instead of t^3 , which would have been the case if they were computed from gyroscopes. In addition, using odometer to compute velocity components eliminate one integration process. Also, since pitch and roll are used to compute velocity, error in position due to error in pitch and roll is proportion to t rather than t^2 (A. Noureldin, 2013). Hence as an alternative, a RISS approach will be beneficial, which limits the accumulation of errors over time (U. Iqbal et al, 2008).

3D-RISS mechanization discussed in this project is demonstrated for land vehicular movement application to obtain a 3-D navigation solution. Since a land vehicle moves mostly in horizontal plane, it makes use of 4 sensors. A gyroscope is placed in z direction of the body. It measures the angular velocity in z direction, used to calculate the Azimuth angle. Two accelerometers are used, one mounted in forwards direction (y -axis), and the other mounted in transverse axis (x -axis). An odometer is used, which is mounted in forward axis, used to measure forward velocity. The two accelerometers compute the pitch and roll angles, which are used to compute velocity components, which, in turn calculate the position components. The IMUs used in this experiment are: IMU300CC-100, a MEMS IMU from Crossbow and a tactical grade IMU from Honeywell, IMU-G2-H58. They will be referred as MEMS IMU and Tactical IMU throughout this literature. To demonstrate the advantages of 3D-RISS mechanization against that of a full IMU mechanization, given trajectory (some samples only) is mechanized for both the cases. Figure 1 illustrates the deviation of position components from the reference at the beginning of mechanization process. 3D-RISS mechanization results followed closely with the

reference. Reference used in this experiment is a Novatel-SPAN unit integrated with Honeywell-IMU-G2-H58.

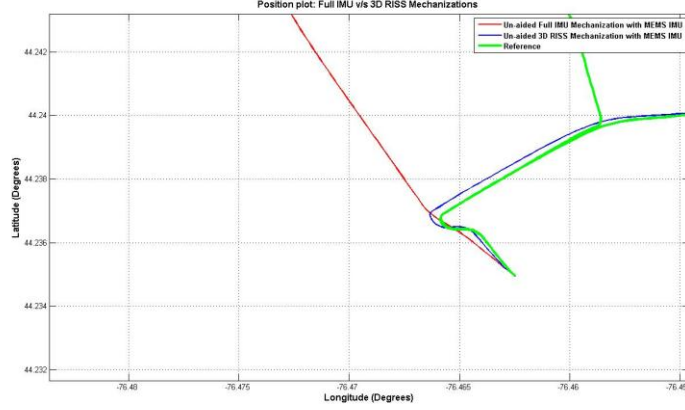


Figure 1 Full mechanization v/s 3D-RISS zoomed-in to show the initial trajectory

3 METHOD

In this section, a set of equations and procedure followed in 3D-RISS mechanization is discussed (Matthew C et al, 2012). X-axis of the body is along the transverse direction, Y-axis is along the forward driving direction, and its Z-axis is along vertical up direction. Local level frame has x, y, z axes along the East, North, and Up directions respectively. All the sensor data represented as f_x and f_y respectively for x and y accelerometers. Z-axis angular velocity is represented as ω_z . The components measured from following set of equations are all represented in local frame.

3.1 Pitch and Roll Computation

Pitch angle is computed after removing forward acceleration (measured from odometer) from f_x . Effect of gravity, which is also measured from f_x and f_y for a small tilt is shown in Figure 2. Similarly roll angle is measured after compensating the normal component of vehicle acceleration from transversal accelerometer, plus the effect of gravity.

$$p = \sin^{-1} \left(\frac{f_y - A_{od}}{g} \right) \quad (1)$$

$$r = -\sin^{-1} \left(\frac{f_x + V_{od}\omega_z}{g \cos(p)} \right) \quad (2)$$

A_{od} is the odometer acceleration, v_{od} is odometer velocity, g is the gravity.

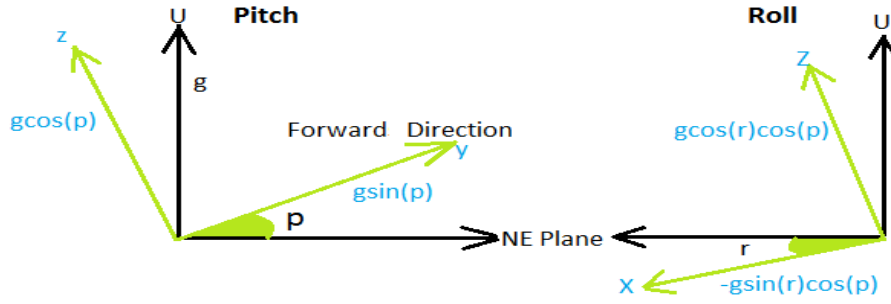


Figure 2 Pitch and Roll realization

3.2 Azimuth Computation

Azimuth (A) is computed from ω_z after compensating for the effect Earth rotation rate (ω^e) and rotation of local frame on the Earth's curvature.

$$\dot{A} = -[\omega_z - \omega^e \sin\varphi - v_e \tan\varphi / (N+h)] \quad (3)$$

v_e is the east velocity, N is normal radius of earth at that point, h is the altitude, and φ is the latitude.

3.3 Velocity Computation

The three velocities along east, north, and up are computed using A , p and v_{od} .

$$v_e = v_{od} \sin A \cos p;$$

$$v_n = v_{od} \cos A \cos p; \quad (4)$$

$$v_u = v_{od} \sin p$$

3.4 Position Computation

Rate of change of position vector is computed from velocity components obtained previously.

$$\begin{pmatrix} \dot{\phi} \\ \dot{\lambda} \\ \dot{h} \end{pmatrix} = \begin{pmatrix} 0 & \frac{1}{M+h} & 0 \\ 1/(\cos\varphi(M+h)) & 0 & 0 \\ 0 & 0 & 1 \end{pmatrix} \begin{pmatrix} v_e \\ v_n \\ v_u \end{pmatrix} \quad (5)$$

M is the meridian radius of earth at that point, λ is the longitude.

3.5 Other RISS Implementation Considerations

Bias and scale factors (SF) of the sensors are to be removed beforehand. Bias and SF are computed in the previous experiment were initially used. However, it is observed that mechanization results implemented using MEMS IMU data as well as tactical IMU data showed large deviation with respect to the reference, as it is evident from the Figure 3. Both the

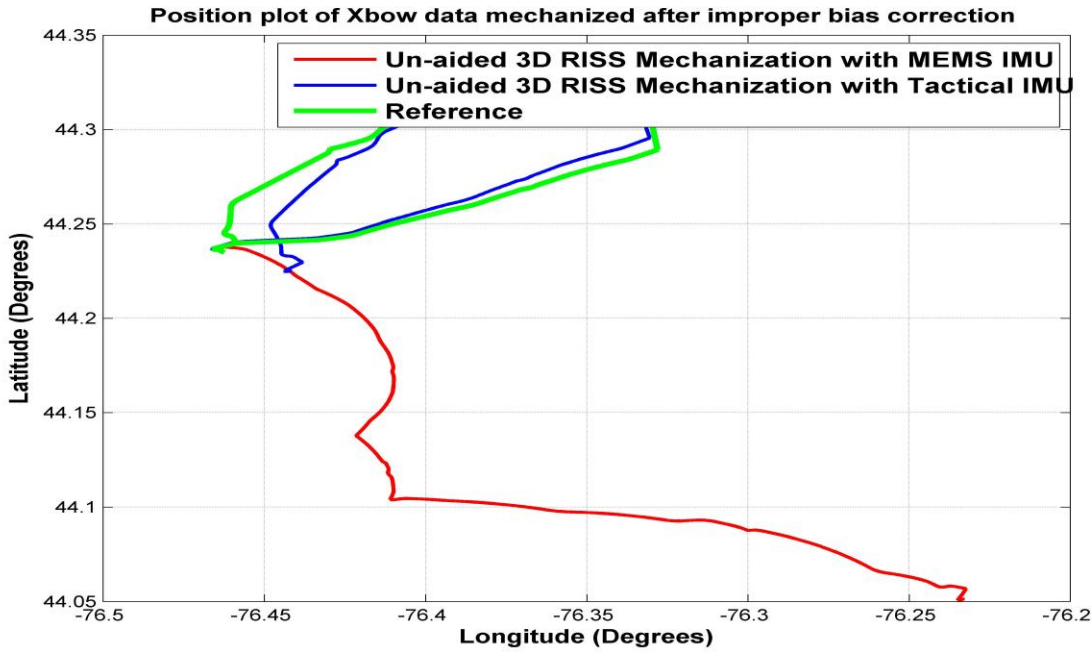


Figure 3 Effect of improper bias and SF

bias and SF need to be tuned to get an acceptable result. The change in the bias from the one computed in Project 1: Calibration of Inertial Sensors may be due to the factors such as temperature change, aging, etc. Fixing the scale factor is important for ω_z as it affects the mechanization at points where sharp turns are involved. Similarly, proper calibration of bias is necessary to avoid the accumulation of errors across various velocity and position components as Azimuth computation is critical in 3D-RISS. Odometer is calibrated by comparing the forward velocity v_{od} with the horizontal component of east velocity and north velocity taken from the reference. Subtracting the two values and averaged over a period of time resulted in approximate bias of 0.2 m/s.

Synchronization is another important aspect of the mechanization. Calibration is followed by the alignment procedure, for which the GPS data are taken as reference. Hence given raw data and reference data needs to be synchronized in order to properly initialize ϕ , λ , h , etc.

It is observed that the tactical IMU raw data were all noisy. Hence, just for the analysis of the scope of this project, IMU data is first de-noised using wavelet function in MATLAB, *when* using the wavelet db5.

The assumption made in this project is that the vehicle mostly moves in horizontal plane, where pitch and roll angle encountered will be very small. Initially when the azimuth computation is implemented as per equation (3), the deviation observed was large. For instance, maximum deviation observed in azimuth with respect to the azimuth from reference is -2.46 degree. When the equation is changed to cater for changes in pitch and roll, as per the below MATLAB code, the maximum deviation was reduced to -2.41 degree. Hence the azimuth is computed in the following way for rest of the analysis.

```
az = -(nova_wz(te)*(cos(p)*cos(r)) - we*sin(phi(te-1)) -  
((v_e(te-1)*tan(phi(te-1)))/(R_N + height(te-1))))*delta_t +  
Azi(te-1)*pi/180;
```

Also, gravity (g), meridian radius (M), and normal radius (N) is computed in every iteration as they are functions of ϕ and h .

4 RESULTS & DISCUSSIONS

The RISS mechanization process is carried out on the data from two types of IMUs, tactical and MEMS grade. Figure 4 shows the 3D trajectory plot for MEMS IMU and tactical IMU, compared with that of reference trajectory. Figure 5 shows the GPS Visualizer (GPS Visualizer, 2013) 2D plot for the same trajectory. It can be observed that performance of tactical IMU is better than the MEMS grade IMU. Position results of mechanizing the tactical IMU are

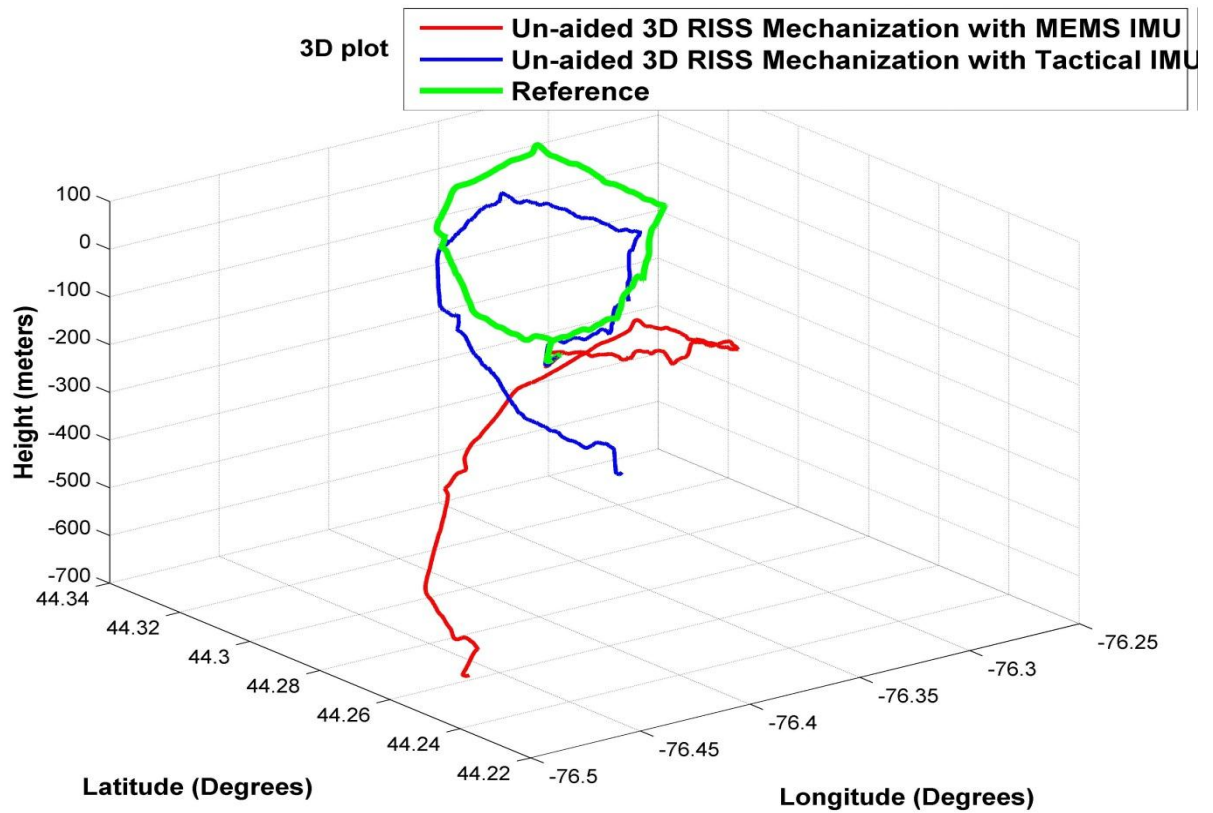


Figure 4 3D plot of RISS Mechanization

deviating away from the reference but the performance of the MEMS is even worse. Latter one's trajectory is deviating slowly away from the reference, ending with a large deviation as the trajectory time increased. It is expected in MEMS as the residual bias in MEMS sensors varies greatly over time.

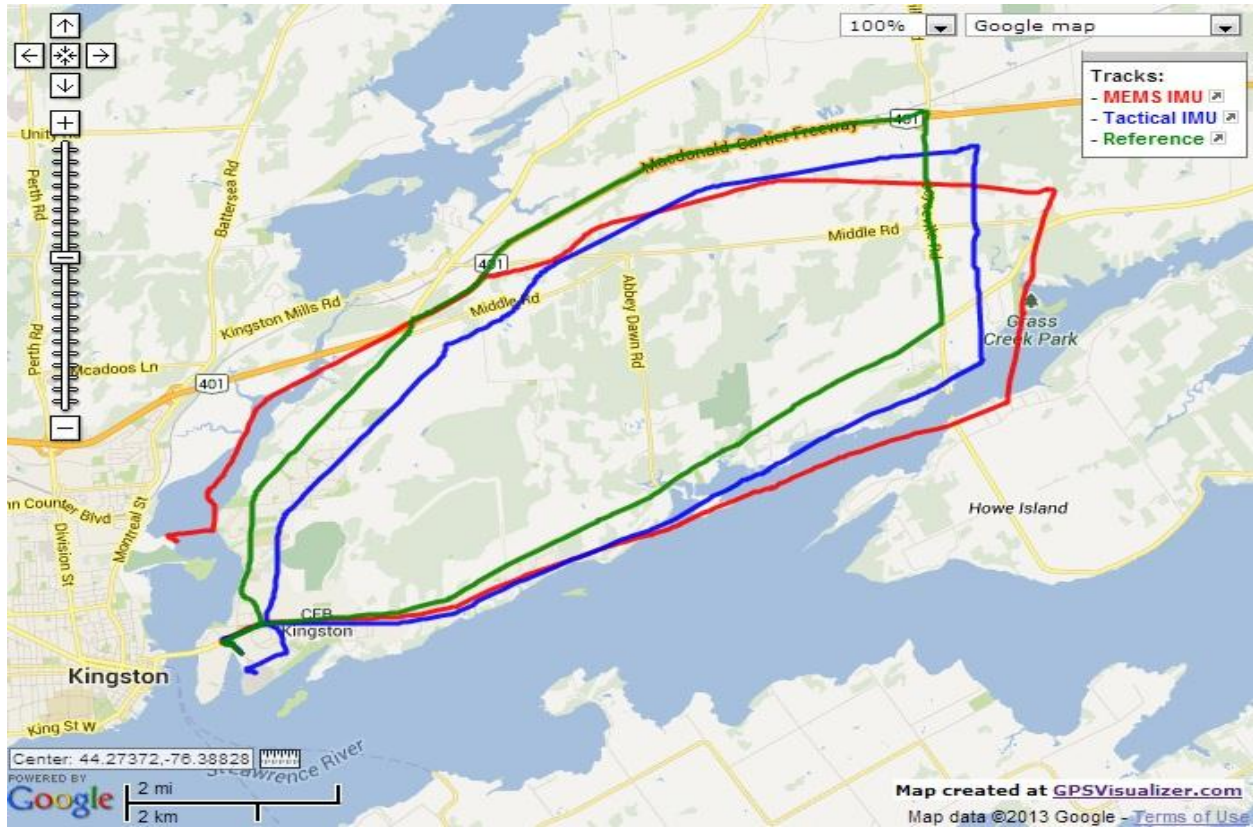


Figure 5 GPS Visualizer 2D plot

As discussed earlier, mechanization for Tactical grade IMU is carried after wavelet de-noising the post calibrated data. The reason for de-noising is discussed in the following. Post calibrated data is initially mechanized to find out the behavior of attitude errors. It is observed that the pitch error is large.

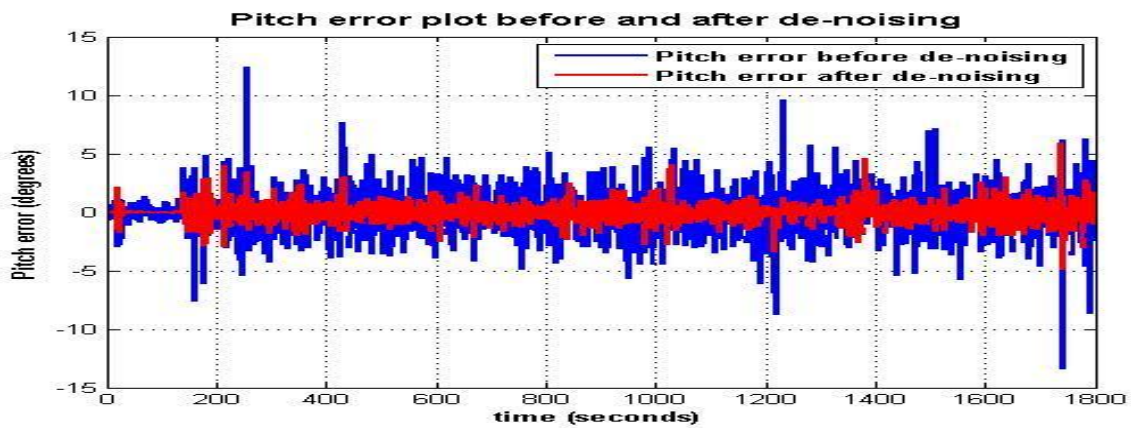


Figure 6 Denoising effect on mechanization

The same data is then de-noised with wavelet db5 and applied for mechanization. The pitch error is reduced significantly as it is evident from Figure 6. Position, velocity and attitude outputs from mechanization of both types of IMUs are discussed in the following. Various types of errors and their possible error sources are investigated.

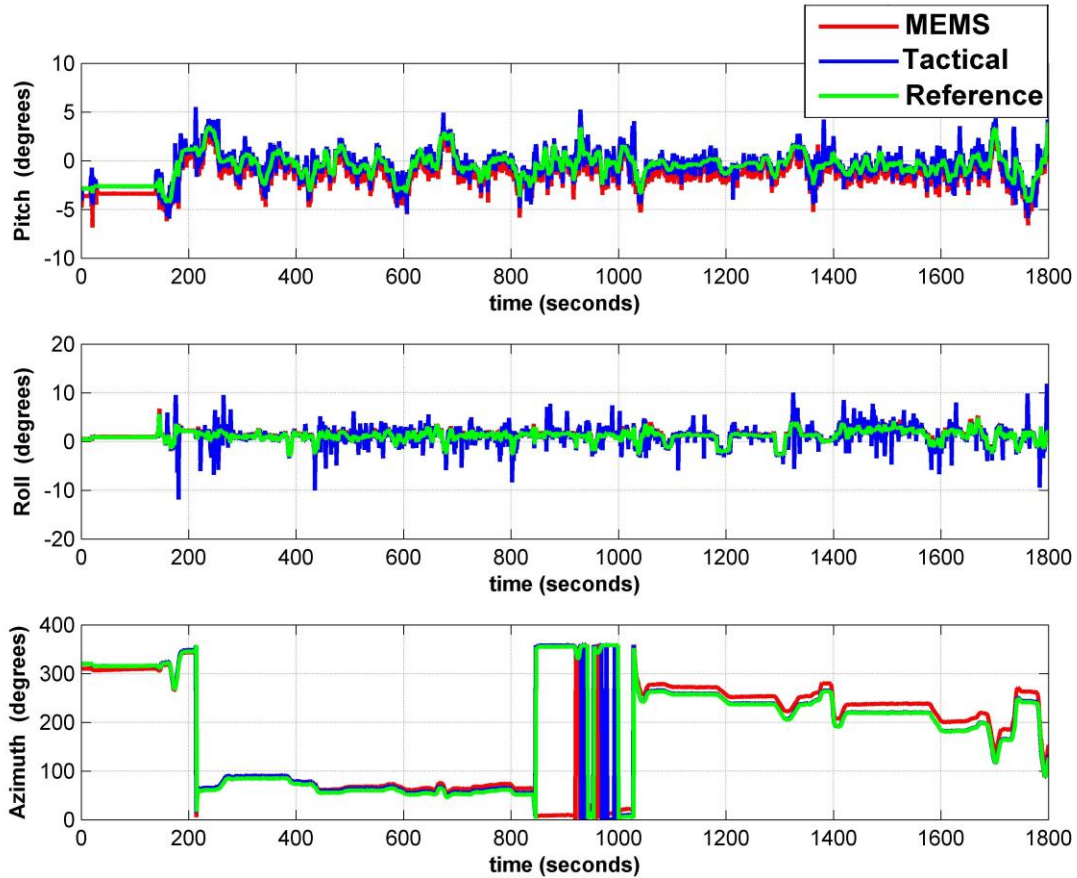


Figure 7 Attitude comparison

Figure 7 is the comparison of attitude computation, which is the first stage in mechanization process. Figure 8 is the attitude error plot for two IMUs, with respect to the reference. Pitch of both IMUs is following the reference, but deviation in MEMS IMU is more as compared to the tactical IMU. This is due to the fact that the bias drift in MEMS IMU sensor is more. Bias drift affects the f_x , and pitch is directly proportional to f_x . Also, other common source of error for both the IMUs could be improper calibration of respective sensors and that of the odometer sensor. It should be noted here that the odometer is not corrected for scale factor due to insufficient data. Roll angle is dependent on ω_z , f_y and pitch. It is observed in the analysis that the contribution of ω_z is significantly large due to its noisy output and improper bias correction. Next

source of error for roll angle is erroneous pitch angle itself. Contribution from f_y is not so significant since the f_y data is less noisy and it is calibrated properly. This was observed after tuning the bias for f_y data.

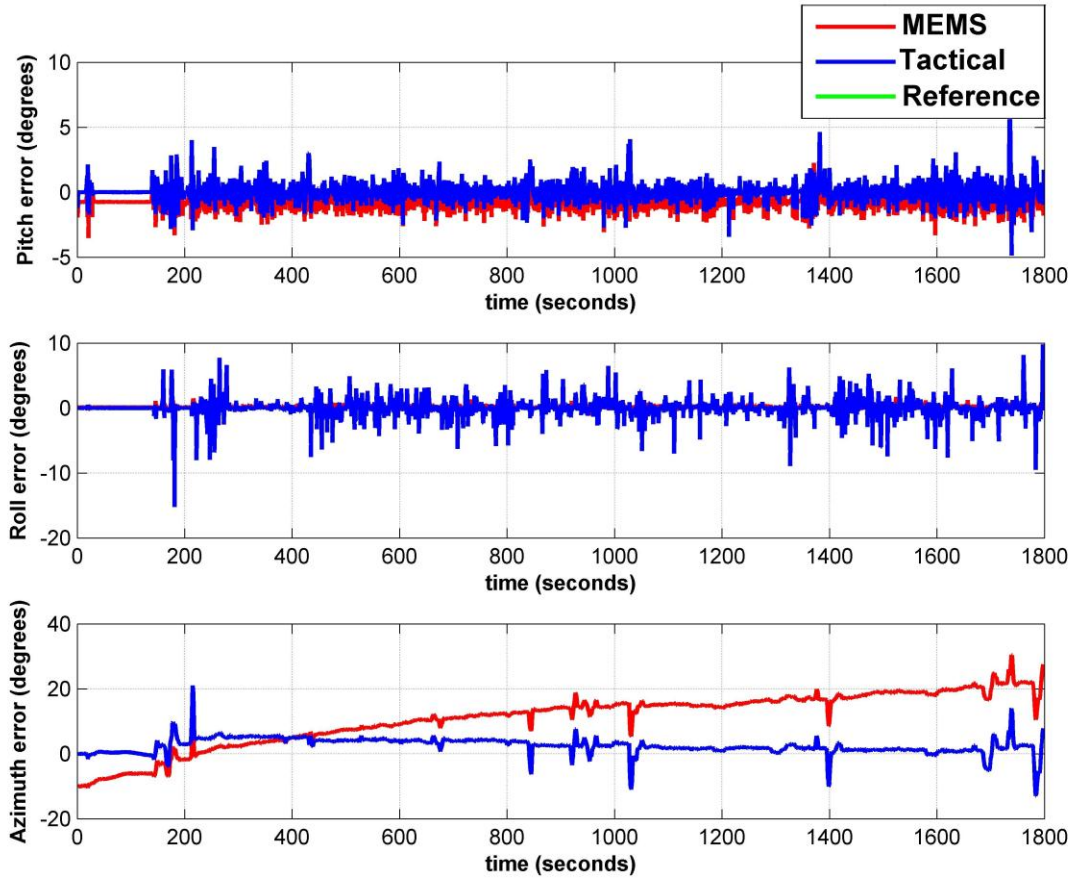


Figure 8 Attitude errors with respect to the reference

Referring to Figure 7, it can be seen that the azimuth of tactical IMU is better compared to that of MEMS IMU, in-terms of following the reference azimuth. Irregular spikes in the overlapped plot are due to the fact that the azimuth is represented in degrees with range from 0 to 360 degrees, which is relatively close to reference near 0 degree Azimuth. To avoid confusion, relative difference in degrees is shown in Azimuth error plot of Figure 8. Important source of error for both IMUs is the ω_z output. Again, in this case also the bias drift rate of MEMS IMU is large compared to that of Tactical IMU, which is the significant contributor to azimuth error. As the time increased, azimuth error of MEMS IMU went on to increase, whereas that of Tactical grade is relatively constant. Spikes in Azimuth error are seen at the places where the vehicle is making large turns. The rate of change in azimuth output is limited by improper scale factor correction of

ω_z . Contribution from east velocity is very small as it is evident from equation (3), due to large denominator factor.

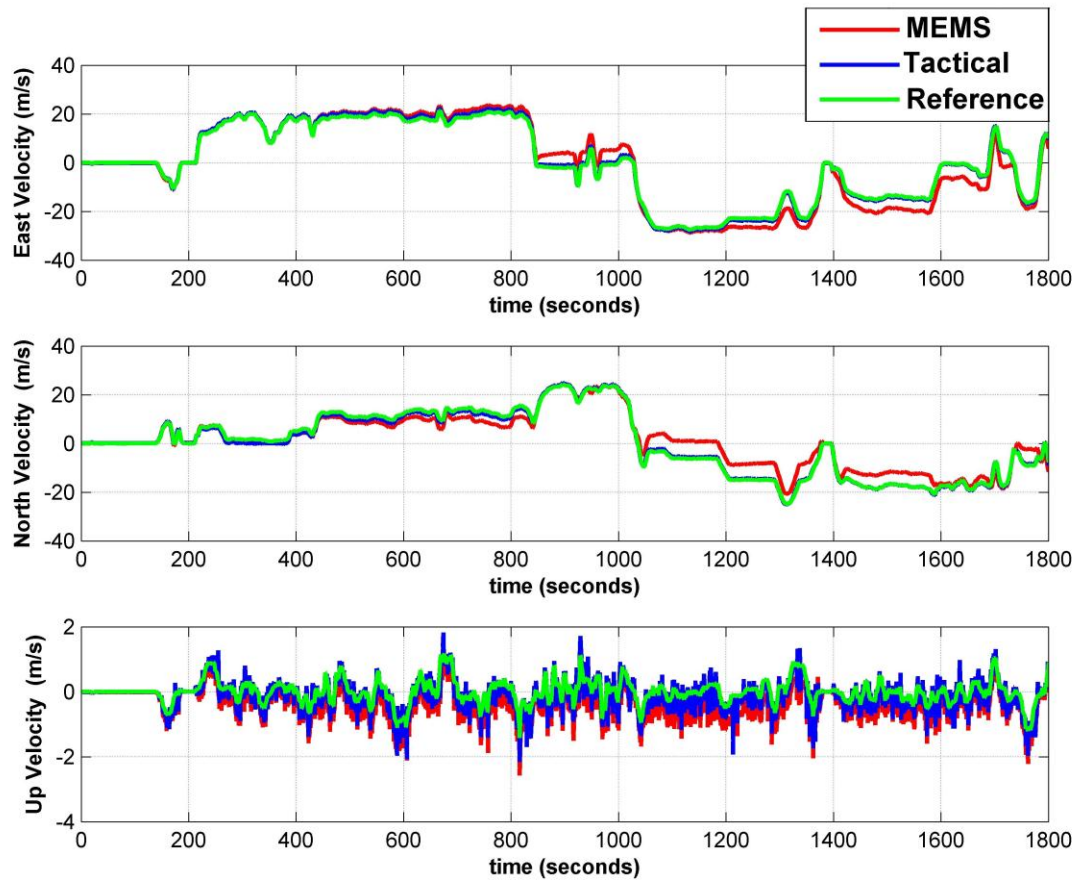


Figure 9 Velocity comparison

Figure 9 shows the velocity comparison. Both east and north velocities follow the reference. Error in east and north are affected the most by error in azimuth. Pitch angle error is also a contributor, which is significant for velocity up, as it is directly proportional to pitch angle. As discussed earlier, odometer is not properly calibrated and its scale factor is not accounted for. From Figure 9, it is evident that Tactical IMU performance is superior to that MEMS IMU. Pitch angle error directly contributes to error in Up velocity as it is illustrated in Velocity Up error plot in Figure 10.

Figure 11 is the comparison of position (latitude, longitude, and height) mechanized from MEMS IMU and Tactical IMU. It shows that the performance of tactical IMU is better than the MEMS IMU. Tactical IMU position has deviated less when compared to the one computed from

MEMS IMU, which is illustrated in Figure 12. It is expected as the east velocity error (proportional to longitude) and north velocity error (proportional to latitude) is less in tactical grade. Altitude in both case, is deviating relatively more than the respective deviations in latitude and longitude. This is because the height is directly proportional to the vertical velocity. Vertical velocity itself is more erroneous due to large pitch errors.

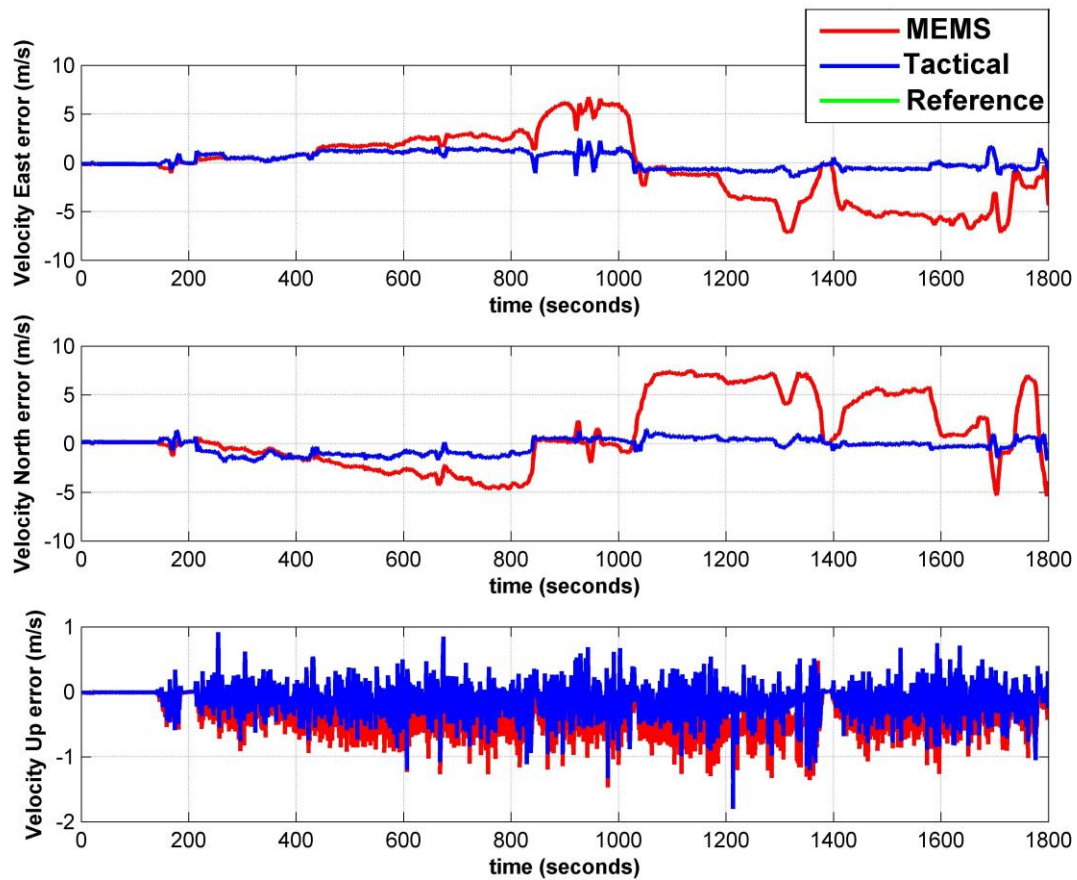


Figure 10 Velocity errors with respect to the reference

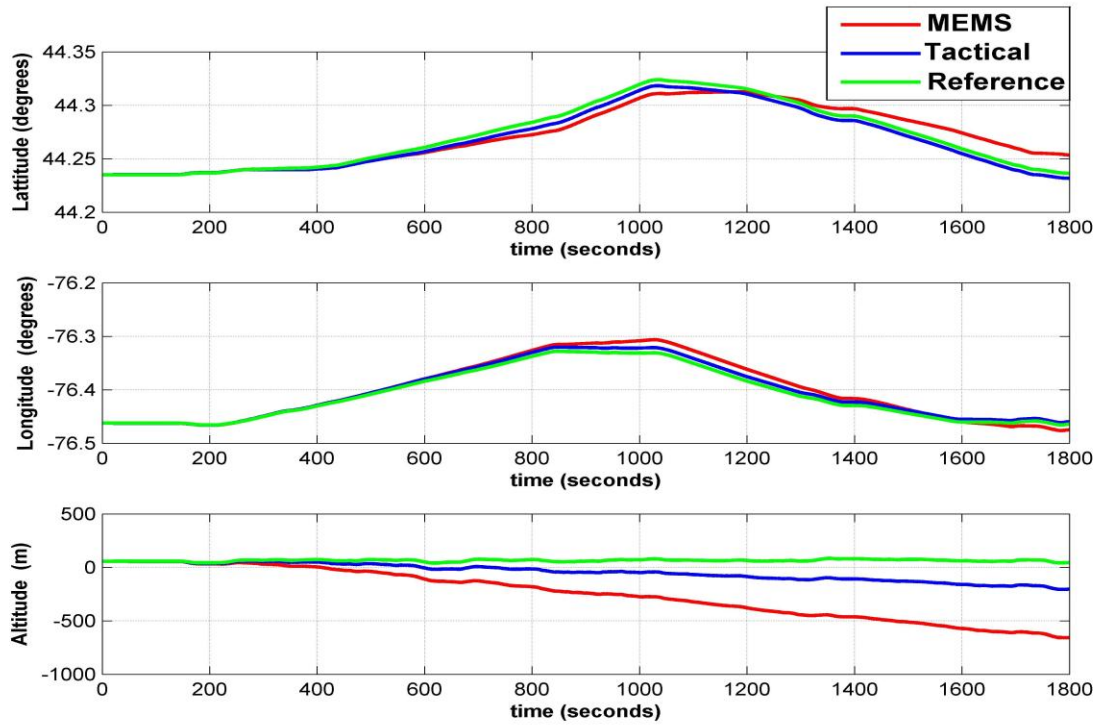


Figure 11 Position comparison

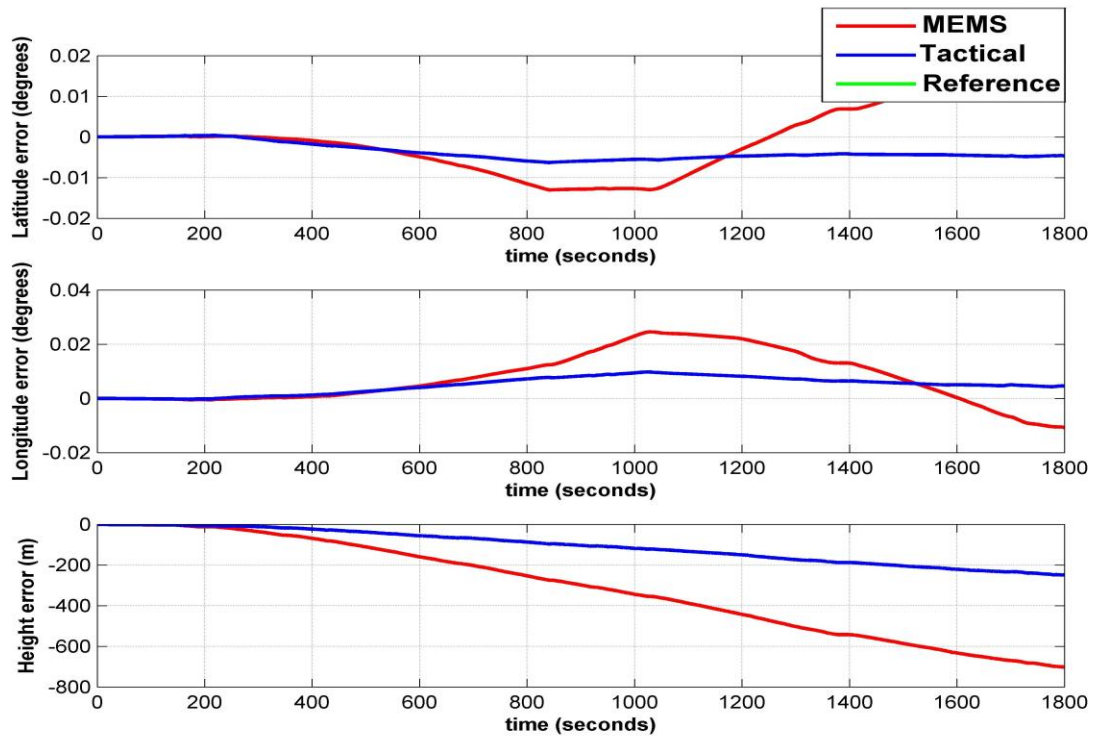


Figure 12 Position errors with respect to the reference

5 CONCLUSIONS

The project discussed drawbacks of full IMU mechanization. As an alternative approach, the process of 3D-RISS mechanization for land vehicular application is discussed. The performance of two types of IMUs, MEMS and tactical grade are compared. Tactical IMU showed superior performance over MEMS grade. Inherent large bias drift rate of MEMS IMU is the key contributor to this effect. Improper calibration of the IMUs (specifically with the gyroscope) and odometer also contributes as an error source. Independent of the grade of the IMU, error associated with mainly with azimuth and, to an extent, pitch propagates in mechanization which results in deviation of position states. Position errors are proportional to vehicle speed, azimuth error, time, and pitch error. These errors can be reduced by modeling the stochastic drift of the sensors in an integration filter.

6 REFERENCES

1. Nouredin, A. (Spring 2013), Inertial Navigation and INS/GPS Integration course, ENGO 623 Course Notes, Department of Geomatics engineering, University of Calgary, Canada
2. Aboelmagd Nouredin, Tashfeen B. Karamat A. Jacques Georgy, (2013), Fundamentals of Inertial Navigation, Satellite-based Positioning and their Integration. ISBN: 978-3-642-30465-1 (Print) 978-3-642-30466-8 (Online)
3. U. Iqbal, A. F. Okou, and A. Nouredin, "An Integrated Reduced Inertial Sensor System—RISS/GPS for Land Vehicle," in *Proceedings of IEEE/ION Position, Location and Navigation Symposium (PLANS '08)*, pp. 1014–1021, Monterey, California, USA, May 2008.
4. <http://www.gpsvisualizer.com/tutorials/tracks.html>, last accessed on June 14, 2013.
5. Matthew Cossaboom, Javques Georgy, Tashfeen B. Karamat, and A. Nouredin , "Augmented Kalman Filter and MapMatching for 3D RISS/GPS Integration for Land Vehicles", in *Hindawi Publishing Corporation International Journal of Navigation and Observation*, Volume 2012, Article ID 567807
6. MATLAB R2012a, Feb 2012, Version 7.14.0739, Help toolbox.
7. U. Iqbal, Tashfeen B. Karamat, A. F. Okou, and A. Nouredin , "Experimental Results on an Integrated GPS and Multisensor Systemfor Land Vehicle Positioning", in *Hindawi Publishing Corporation International Journal of Navigation and Observation*, Volume 2009, Article ID 765010